

**PHASE SPACE CHARACTERISTICS OF FRAGMENTING
NUCLEI DESCRIBED AS EXCITED DISORDERED SYSTEMS**

J. Richert, D. Boosé, A. Lejeune*

Laboratoire de Physique Théorique, Université Louis Pasteur,
3, Rue de l'Université, 67084 Strasbourg Cedex, France

and

P. Wagner

Centre de Recherches Nucléaires, IN2P3/CNRS and Université Louis Pasteur,
BP28, 67037 Strasbourg Cedex 2, France

Abstract

We investigate the thermodynamical content of a cellular model which describes nuclear fragmentation as a process taking place in an excited disordered system. The model which reproduces very well the size distribution of fragments does not show the existence of a first order phase transition.

* On leave of absence from the Laboratoire de Physique Nucléaire Théorique, Institut de Physique B5, Université de Liège, B-4000 Sart Tilman, Liège, Belgium.

1. Introduction

The description and understanding of nuclear fragmentation has remarkably progressed during these last years. There remains nevertheless a long standing question for which no completely satisfactory answer has yet been found. It concerns the existence of an energy triggered signal which would reveal the existence of a phase transition in nuclear matter.

Among the advances which have come out through the confrontation of experimental measurements [1-5] with theoretical investigations one may mention the behaviour of final fragment charge distributions. They show that the fragmentation process leads to universal properties which can be interpreted in the framework of very simple descriptions [6]. In particular, the interpretation of percolation analyses points towards the existence of a second order phase transition which takes place in an excited disordered system [7-8]. More recently, experimental data [9] were used in order to relate the excitation energy to a temperature which characterises the fragmenting system produced in peripheral collisions. The caloric curve which comes out of these data shows a typical plateau in temperature, with some kind of up-swing on the lower side of the energy interval over which the effect is observed. Whether this result and its interpretation will be definitely confirmed or not is, at present, an open question. First, it has to be cross-checked that the temperature which was obtained by means of a model [10] is consistent with other experimental methods aimed to fix this quantity. Up to now, this is not clear [11]. Second, the concept of temperature itself makes sense only if the system is in thermodynamical equilibrium which is tacitly supposed to be realised, although it can never be rigorously so. Indeed, one expects the presence of more or less strong non-equilibrium features like collective flow, even in peripheral kinematics. This point has to be kept in mind when a comparison between theoretical model calculations and experimental results is performed.

Many different theoretical models have been proposed in order to describe nuclear fragmentation. The specific question concerning the thermodynamic properties of fragmenting nuclei and the possible existence of different phases has been investigated by means of time-dependent approaches [12-14] as well as thermodynamic equilibrium models which describe the freeze-out stage of the process in the framework of the canonical [16] and the microcanonical ensembles [15]. Both of these last calculations lead to a caloric curve which shows the characteristic behaviour of a first order phase transition taking place in a finite system. This may

be interpreted as a support of the experimental result, although, as already stated, it is not clearly established that the physical conditions which are experimentally realised are those introduced by the models.

In a former work [7,8] we proposed a classical microscopic description in which a fragmenting nucleus is an excited and disordered system. The approach is able to reproduce the results of bond percolation as well as the ALADIN data [17,18] concerning charge distributions of fragments and related observables. This success legitimates the interest in further phase space properties of the model. In particular, it is worthwhile to see whether it can or cannot reproduce the thermodynamic properties predicted by the recent experiments.

The organisation of the present paper is the following. In section 2 we first recall the essential features of our approach and describe the way we construct a partition function of the system in the framework of the microcanonical ensemble (fixed energy). We discuss the way through which we establish the correspondence between the energy and a temperature and present the results of our numerical investigations. In section 3 we develop an analytical version of our approach which we confront with the numerical findings. We discuss our results and draw conclusions in section 4.

2. Description of a disordered and excited system of particles and its thermodynamical properties

2.1 Cellular model approach to nuclear fragmentation

We start with the description of the model which has already been introduced in Refs. [7,8]. We consider a finite compact volume V in 3-dimensional space, in practice a cube. This volume is divided into A equal cubic cells of linear dimension d . Each cell is occupied by a classical particle, i.e. $V = Ad^3$. Each particle i is characterized by its phase space coordinates, i.e. its position \vec{r}_i with respect to the centre of mass of the system and its linear momentum \vec{p}_i . The coordinates (x_i, y_i, z_i) are chosen as $x_i = x_{i_0} + \varepsilon d/2$ and similarly for y_i and z_i . The coordinate $\vec{r}_{i_0}(x_{i_0}, y_{i_0}, z_{i_0})$ corresponds to the centre of the cell and ε is a random number drawn from a distribution which, in practice, is chosen to be uniform in the interval $[0,1]$. The momenta \vec{p}_i are drawn randomly and uniformly in a sphere of arbitrary large radius p_{\max} . We introduce the maximum kinetic energy of a particle as $E_{\max} = p_{\max}^2/2m$.

The particles interact by means of two-body interactions. In practice we in-

roduce a strong short range nuclear potential. For reasons of consistency with former calculations [8] we essentially use the interaction of Ref. [19] which does not explicitly differentiate protons and neutrons. If we select another potential in the sequel we shall mention it in due place. We choose part of the nucleons to be protons which we distribute uniformly in cells over the whole space and implement the Coulomb potential which acts between charged particles. The potential energy of the system is obtained by adding up the interaction energy between the particles. We have also considered the case where the nuclear interaction is restricted to nearest neighbours. This approximation changes absolute values of energies but does not affect the conclusions which will be drawn below.

Former use of this classical approach has nicely proven that the present description of excited fragmenting nuclear systems is able to reproduce the fragment size distributions and related observables which are obtained in the framework of ordinary bond percolation [7,8]. The calculations show that the results are very robust with respect to the explicit choice of the interaction, the shape of the external surface of the system and even the criteria which are used in order to define bound systems of particles, i.e. fragments.

2.2 Thermodynamical aspects

2.2.1 Motivations

The agreement between percolation calculations which are generic for the description of disordered systems and experimental results suggests a possible interpretation of fragmentation as a critical phenomenon, more precisely a second order phase transition in presence of finite size effects since it takes place in a small system. A recent interpretation of experimental data raises a new question. Indeed, the determination of the temperature of the excited fragmenting system and the knowledge of the excitation energy of projectile-like nuclei formed in peripheral collisions lead to a caloric curve which exhibits the characteristic plateau corresponding to latent heat generation. This effect which is seen in infinite systems undergoing a first order phase transition is interpreted as a liquid-gas-like transition [9]. This result which as already said, is still under critical investigation and its interpretation led us naturally to the question as to whether our approach can reproduce such an effect or not. This is the point we want to present and discuss in the sequel.

2.2.2 Generation of microcanonical configurations

The total number of configurations which can be generated for a fixed energy

E , number of particles A and volume $V = Ad^3$ is designated by $Z(E, A, d)$, the microcanonical partition function of the system when it is in thermodynamical equilibrium.

In practice we construct this quantity numerically in the following way. We generate N configurations with our cellular model as described above and calculate the potential energy of the system by summing up the two-body interaction energy which acts between all pairs of particles of the system, i.e. the nuclear and the Coulomb contributions. The number Z of charged particles is such that Z/A corresponds to nuclei energetically located in the valley of stability. Doing this way we obtain N configurations with potential energy $\{E_{pot}^{(k)}, k = 1, \dots, N\}$.

In a second step we generate a set of configurations for which we determine the kinetic energy content. For each configuration we choose randomly p_{\max} (see above) out of a uniform distribution in an interval $[0, P_{up}]$ where P_{up} is an upper limit for the momenta which we fix arbitrarily. We then draw randomly, for fixed p_{\max} , an ensemble of momenta $\{|\vec{p}_i|, i = 1, \dots, A\}$ in the Fermi sphere of radius p_{\max} as already described above. Proceeding this way we generate a set of events with total kinetic energy $\{E_{kin}^{(k)}, k = 1, \dots, N\}$. The number of events is generally of the order of 10^6 .

We fix then the total energy of the system to lie in bins $[E, E + \Delta E]$ and count the number of configurations which correspond to a total energy $E = E_{kin} + E_{pot}$ lying in this bin by means of the combination of the kinetic and potential energy configurations which were generated as described above. The number of configurations which are found gives the partition function $Z(E, A, d)$. This is done for all energies which the system can reach, from a minimum value E_{\min} to the maximum which is $E_{up} = A \cdot P_{up}^2/2m$. E_{up} is necessarily a finite quantity because it is necessary to define a finite upper bound in numerical simulations. This leads to the fact that $Z(E, A, d)$ may start to decrease for the higher values of E . This is an unphysical effect. Hence we must restrict the further use of the partition function to an interval of energy which does not take its high energy tail into account.

2.2.3 Thermodynamical analysis of the disordered system. Results

The knowledge of the microcanonical partition function leads to the entropy $S(E, A, d)$ and the temperature through

$$T^{-1} = (\partial S / \partial E)_V \tag{1}$$

which establishes the relationship between T and E , i.e. the so called caloric curve.

We have determined $Z(E, A, d)$ for different values of d , i.e. different total volumes. In order to work out the derivative of $S = \ln Z$ we have introduced an analytical parametrisation of S over the whole range of values in terms of Chebyshev polynomials of different orders. Using statistically significant samples of configurations (of the order of 10^6) it is possible to approximate S with an excellent precision ($\chi^2 \leq 1$). Fig. 1a shows the behaviour of Z obtained by means of the numerical simulations described above and the result of the analytical fit which is practically indistinguishable from the numerical result. The corresponding caloric curve is represented in Fig. 1b. There is no sign for the existence of a plateau in the temperature which would signal a first order phase transition.

In Fig. 2 we present the behaviour of $(\partial S / \partial E)_V^{-1}$ for different values of V which correspond to values of d in the interval $[1.8, 4]$ fm (average densities ρ in the interval $[0.016, 0.17]$ fm $^{-3}$). One observes a strong dispersion of the curves as a function of the energy which indicates that this quantity is sensitive to the volume in which the system moves. The large negative energy thresholds come from the fact that the nucleon potential we chose [19] and which was also used in Refs. [7,8] overbinds heavy systems (here $A = 216$). In our former study of fragment size distributions [7,8] we mixed up events which correspond to systems of different sizes. Since, for different experimental events, the nucleus may break up into fragments at different densities it is tempting to collect in a uniform way events corresponding to different values of d . This is what we did in order to construct an ‘‘entropy’’ which is averaged over different values of d , $\langle S \rangle_d$. In Fig. 2 we show the behaviour of $(\partial \langle S \rangle_d / \partial E)_V^{-1}$ (dotted line). Again, this quantity shows a monotonous rise with the energy.

We also used the potential defined in Ref. [20] which differentiates protons and neutrons and hence leads to a quite different energy dependence of the system. As it can be seen in Fig. 3 one finds the same behaviour of the observables as in the former case.

2.2.4 Comments

We comment and discuss now the results obtained above. First, the fact that we take together events corresponding to different volumes violates (1) since $\partial S / \partial E$ must be calculated for fixed volume. The only way out is to say that the quantity which corresponds to $(\partial \langle S \rangle_d / \partial E)^{-1}$ is some effective temperature. It is

not clear whether it could be put in connection with temperatures related to the experimental situation where the fragmentation may go on in a variable volume.

Second, it is interesting to confront the behaviour of the partition sum $Z(E, A, d)$ with the multiplicity as a function of increasing energy. This is shown in Fig. 4. As expected there exists a clear correspondence between the increase of the number of configurations and the increase of the number of fragments and particles over the whole energy range. However this connection is not related to a phase transition, as already stated above (no exponential increase of $Z(E, A, d)$ over a finite energy interval in which one would observe a coexistence of fragments and particles).

Last, thermodynamical equilibrium which is a prerequisite for the use of (1). There is no reason why all the configurations we generate should correspond to such a situation since we do not implement a Metropolis Monte Carlo type algorithm in order to select those configurations which correspond to equilibrium. We try now to eliminate the problem concerning thermodynamical equilibrium by implementing an analytical approach.

3. Analytic approach to the description of an excited disordered system

As previously discussed, the numerical simulations which were performed above do not necessarily generate an equilibrated system. It raises the questions whether the outcome of our model would be different if this property would be satisfied. This should be done by implementing some Metropolis Monte Carlo algorithm. Such calculations may be done in the future. Here we try to work out an analytical model which guarantees thermodynamic equilibrium. Furthermore, its geometric and dynamical properties are very close to those of the system which has been investigated above. We want to check the effects of possible deviations from equilibrium which is not realised in the calculations of section 2.

3.1 Derivation of the canonical partition function

We construct the canonical partition function of a set of A classical particles in thermodynamic equilibrium at a temperature $T = \beta^{-1}$. The particles are distributed in A identical cells of linear dimension d . As before, there is one particle in each cell. Then

$$\tilde{Z}(\beta, A, d) = \sum_{\mathcal{C}(\{\vec{r}_i, \vec{p}_i\})} e^{-\beta H(A, d)} \quad (2)$$

$$= \prod_{i=1}^A \int_{V_{p_i}} d\vec{p}_i \int_{V_{r_i}} d\vec{r}_i e^{-\beta H(\{\vec{r}_i, \vec{p}_i\})}$$

with

$$H(\{\vec{r}_i, \vec{p}_i\}) = \sum_{i=1}^A \frac{p_i^2}{2m} + \sum_{i<j} V(|\vec{r}_i - \vec{r}_j|)$$

V_{p_i} and V_{r_i} are the volumes occupied by a particle in a phase space cell. We consider first a 1-dimensional system for which cells are segments of length d . The potential V is defined in terms of a truncated harmonic oscillator which acts between neighbouring particles i and j located at x_i, x_j such that

$$\begin{aligned} V &= \infty & |x_i - x_j| < r_c \\ &= V_0 + C(x_i - x_j)^2 & r_c \leq |x_i - x_j| \leq r_0 \\ &= 0 & |x_i - x_j| > r_0 \end{aligned}$$

The parameter r_c introduces a hard core. The effective range of the interaction r_0 is chosen to be of the order of $2d$. The strength V_0 is negative and $C = -V_0/r_0^2$.

The potential V is aimed to simulate a realistic short range nuclear potential which is attractive and strongly repulsive at short distances.

The model can be easily extended to 3 dimensions (see below). It is expected to be qualitatively close to the more realistic potentials used in numerical simulations. The long range Coulomb interaction is not taken into account. From our numerical experience this should not alter our conclusions.

3.2 Kinetic and potential contributions to the partition function

The kinetic contribution is trivially given by

$$\tilde{Z}_{kin}(\beta, A) = \prod_{i=1}^A \int_{-\infty}^{+\infty} dp_i \exp(-\beta p_i^2/2m) = (2\pi m/\beta)^{A/2} \quad (3)$$

The potential contribution can also be worked out explicitly. The potential energy reads

$$V = AV_0 + C [(x_1 - x_2)^2 + \dots + (x_{A-1} - x_A)^2 + (x_A - x_1)^2]$$

We impose periodic boundary conditions

$$x_{A+1} = x_1$$

and introduce new coordinates

$$x_i = x_i^0 + \delta x_i \quad ; \quad \delta x_{A+1} = \delta x_1$$

where x_i^0 defines the centre of the interval i .

Then

$$V = AV_0 + ACd^2 + C \sum_{i=1}^A (\delta x_{i+1} - \delta x_i)^2 + 2Cd \sum_{i=1}^A (\delta x_{i+1} - \delta x_i)$$

The periodic boundary condition eliminates the last term on the right hand side. Hence the potential contribution to the partition function reads

$$\tilde{Z}_{pot}(\beta, A, d) = \exp[-\beta A(V_0 + Cd^2)] \cdot \prod_{k=1}^A \int_{-b}^b d\delta x_k \exp\left[-\beta C \sum_{i=1}^A (\delta x_{i+1} - \delta x_i)^2\right]$$

where $[-b, +b]$ with $b = d/2 - r_c$ is the range over which δx_i can vary in the interval i .

The exponent of the integrand in \tilde{Z}_{pot} is a quadratic form which corresponds to a matrix with A equal diagonal elements $2\beta C$, two symmetrical subdiagonals with equal elements $-\beta C$ and two elements $-\beta C$, one in the upper right corner and one in the lower left corner. This “tight-binding” matrix can be explicitly diagonalised and the eigenvalues are given by

$$\tilde{\lambda}_i = 2\beta C \left(1 - \cos\left(\frac{2\pi i}{A}\right)\right) = \beta C \lambda_i \quad (i = 1, \dots, A)$$

The lowest eigenvalue corresponds to $\tilde{\lambda}_A = 0$. The other eigenvalues are degenerate of order 2, $\tilde{\lambda}_{A-i} = \tilde{\lambda}_i$. If A is even, the eigenvalue $\tilde{\lambda}_{A/2} = 4\beta C$ is the largest and it is non degenerate.

It is also possible to work out the expression of the eigenvectors and to obtain the new boundaries in the new variables $\{\delta X_i\}$ corresponding to the rotated system and associated with the eigenvalues $\{\tilde{\lambda}_i\}$.

For A odd one gets

$$-b\sqrt{A} \leq \delta X_1 \leq +b\sqrt{A} \quad \text{corresponding to } \lambda_A$$

and

$$\begin{aligned} -b_i &\leq \delta X_{2i} \leq +b_i \\ -c_i &\leq \delta X_{2i+1} \leq +c_i \end{aligned}$$

where

$$b_i = b \sqrt{\frac{2}{A}} \left(1 + 2 \sum_{k=1}^{\frac{A-1}{2}} \left| \cos \left(\frac{2\pi k}{A} \cdot i \right) \right| \right)$$

$$c_i = b \sqrt{\frac{2}{A}} \left(1 + 2 \sum_{k=1}^{\frac{A-1}{2}} \left| \sin \left(\frac{2\pi k}{A} \cdot i \right) \right| \right)$$

which correspond to the degenerate eigenvalue λ_i .

For A even the boundaries are

$$-b \sqrt{A} \leq \delta X_{1,2} \leq +b \sqrt{A}$$

corresponding to λ_A and $\lambda_{A/2}$

and

$$\begin{aligned} -b_i &\leq \delta X_{2i+1} \leq +b_i \\ -c_i &\leq \delta X_{2i+2} \leq +c_i \end{aligned}$$

corresponding to the degenerate eigenvalues λ_i . Here b_i and c_i are the same as those given above, except that the upper limit of the sums corresponds now to $k = A/2 - 1$.

As a consequence of these developments the expression of \tilde{Z}_{pot} can be explicitly integrated for finite A . For A odd one gets

$$\begin{aligned} \tilde{Z}_{pot}^{(o)}(\beta, A, d) &= \exp[-\beta A(V_0 + Cd^2)] \cdot 2b A^{1/2} \cdot (\pi/\beta C)^{(A-1)/2} \\ &\cdot \left(\prod_{i=1}^{(A-1)/2} \lambda_i \right)^{-1} \cdot \prod_{i=1}^{(A-1)/2} \left\{ \operatorname{erf}[(\beta C \lambda_i)^{1/2} b_i] \cdot \operatorname{erf}[(\beta C \lambda_i)^{1/2} c_i] \right\} \end{aligned} \quad (4a)$$

and for A even the expression reads

$$\begin{aligned} \tilde{Z}_{pot}^{(e)}(\beta, A, d) &= \exp[-\beta A(V_0 + Cd^2)] \cdot 2b A^{1/2} \cdot (\pi/\beta C \lambda_{A/2})^{1/2} \cdot (\pi/\beta C)^{(A-2)} \\ &\cdot \left(\prod_{i=1}^{(A-2)/2} \lambda_i \right)^{-1} \cdot \prod_{i=1}^{A/2-1} \left\{ \operatorname{erf}[(\beta C \lambda_i)^{1/2} b_i] \cdot \operatorname{erf}[(\beta C \lambda_i)^{1/2} c_i] \right\} \end{aligned} \quad (4b)$$

where $\operatorname{erf}(x)$ is the error function and $\lambda_i = \tilde{\lambda}_i/\beta C$ ($i = 1, \dots, A$).

3.3 Approximate expressions

It is now possible to write down $\tilde{Z}(\beta, A, d)$ as the product of $\tilde{Z}_{kin}(\beta, A)$ given by (3) and $\tilde{Z}_{pot}(\beta, A, d)$ given by (4a) or (4b). This is however of no practical use since it would not allow us to get an explicit expression of the microcanonical partition function $Z(E, A, d)$ which we would like to confront with our simulation results.

For this reason we introduce an approximation in our calculation of \tilde{Z}_{pot} . In practice, we replace the rotated hypercube which defines the volume in which the $A - 1$ rotated coordinates $\{\delta X_i\}$ vary by a hypersphere whose radius R is defined in such a way that its volume is the same as that of the original hypercube of dimension $A - 1$ (the coordinate corresponding to $\lambda_A = 0$ is not taken into account).

This procedure leads to

$$R = [V \cdot \Gamma(A + 1)/2]^{1/(A-1)}/\pi^{1/2} \quad (5)$$

where $V = (2b)^{(A-1)} \cdot \left(\prod_{k=1}^{(A-1)/2} \lambda_k \right)$ for A odd.

If we introduce this approximation we get the partition function

$$\begin{aligned} \bar{Z}_{pot}^{(o)}(\beta, A, d) = & \exp[-\beta A(V_0 + Cd^2)] \cdot 2b A^{1/2} \cdot (\pi/\beta C)^{(A-1)/2} \\ & \cdot \left(\prod_{i=1}^{(A-1)/2} \lambda_i \right)^{-1} \cdot \left[1 - \exp(-\beta CR^2) \sum_{m=0}^{(A-3)/2} \frac{(\beta CR^2)^m}{m!} \right] \end{aligned} \quad (6a)$$

for the case where A is odd, and

$$\begin{aligned} \bar{Z}_{pot}^{(e)}(\beta, A, d) = & \exp[-\beta A(V_0 + Cd^2)] \cdot 2b A^{1/2} \cdot (\pi/\beta C \lambda_{A/2})^{1/2} \cdot (\pi/\beta C)^{(A-2)} \\ & \cdot \operatorname{erf} \left[b A^{1/2} (\beta C \lambda_{A/2})^{1/2} \right] \cdot \left(\prod_{i=1}^{(A-2)/2} \lambda_i \right)^{-1} \cdot \left[1 - \exp(-\beta CR^2) \sum_{m=0}^{(A-4)/2} \frac{(\beta CR^2)^m}{m!} \right] \end{aligned} \quad (6b)$$

for the case where A is even. In (6b) R is defined by (5), but $A - 1$ is replaced by $A - 2$.

The exact and approximate expressions \tilde{Z}_{pot} and \bar{Z}_{pot} are close and it is easy to guess that their behaviour as a function of β is qualitatively similar. We have

checked this point by means of explicit numerical calculations in which we compare the product of error functions appearing in (4a) and (4b) with the R -dependent terms in (6a) and (6b). Calculations done for different values of A and different choices of parameters are shown in Fig. 5 for the quantities by which $\tilde{Z}^{(o)}$ and $\bar{Z}^{(o)}$ given by (4a) and (6a) differ (last terms of the expressions). The results show that these quantities have the same monotonous behaviour, with the same limit as β goes to infinity. In both cases the derivatives of the curves go to zero as β goes to zero.

3.4 Microcanonical partition function

We use \bar{Z} in order to construct the microcanonical partition function by means of an inverse Laplace transform

$$Z(E, A, d) = \frac{1}{2\pi i} \int_{c-i\infty}^{c+i\infty} d\beta e^{\beta E} \bar{Z}(\beta, A, d) \quad (7)$$

Because of the explicit dependence of \bar{Z} on β it is possible to work out Z explicitly.

It should be noticed here that inverse Laplace transforms can be highly unstable quantities [21,22]. This fact is particularly troublesome when $Z(\beta)$ is numerically determined since any deviation of $Z(\beta)$ can produce important deviations of $Z(E)$ from its real value. In our case $\tilde{Z}(\beta)$ is known analytically. We believe that, even though $\bar{Z}(E)$ we obtain from this analytic expression is not the same as the exact one, $\bar{Z}(E)$ reflects the qualitative behaviour of the exact partition function $\tilde{Z}(E)$ because of the analytical behaviour of both functions $\tilde{Z}(\beta)$ and $\bar{Z}(\beta)$ (see above and Fig. 5). This is sufficient in order to conclude confidently about the qualitative behaviour of E vs. T (see below and Figs. 6 and 7).

Using (6a) it is straightforward to show that

$$\begin{aligned} Z(E, A, d) &= (2\pi m)^{A/2} (\pi/C)^{(A-1)/2} \cdot 2bA^{1/2} \cdot \left(\prod_{k=1}^{A-1} \lambda_k^{1/2} \right)^{-1} \\ &\cdot \left\{ \frac{[(E - A(V_0 + Cd^2))]^{A-3/2}}{\Gamma(A-1/2)} \cdot \Theta[E - A(V_0 + Cd^2)] \right. \\ &- \sum_{m=0}^{(A-3)/2} \frac{C^m R^{2m}}{m! \Gamma(A-m-1/2)} [E - A(V_0 + Cd^2) - CR^2]^{A-m-3/2} \\ &\left. \cdot \Theta[E - A(V_0 + Cd^2) - CR^2] \right\} \quad (8) \end{aligned}$$

where R has been defined above. This expression shows explicitly that $Z(E, A, d)$ has an algebraic dependence on E starting from a threshold energy $E = A(V_0 + Cd^2)$. There is no sign for an exponential behaviour which would indicate the existence of a plateau in the $(T = \beta^{-1}, E)$ representation. The fact that Z is a monotonic increasing algebraic function of E is confirmed by numerical tests of expression (8), see Fig. 6. This confirms and comforts the results obtained through simulations in section 2.

The analytic results can easily be extended to a 3-dimensional system since, because of the choice of the two-body potential, the potential contribution factorises in the 3 space dimensions (x, y, z) . Hence the expressions are formally similar to those obtained in the 1-dimensional case, except for the eigenvalue spectrum $\{\lambda_k; k = 1, \dots, A\}$ which is affected by the dimensionality of the total space because, in the nearest-neighbour interaction approximation the coordinance goes over from 2 in the 1-dimensional case to 6 in the 3-dimensional one. The partition function reads now explicitly

$$\begin{aligned}
Z(E, A, d) &= (2\pi m)^{3A/2} \cdot (2bA^{1/2})^3 \cdot (\pi/C)^{(A-1)/2} \left(\prod_{i,j,k=1}^{A-1} \lambda_{i,j,k}^{1/2} \right)^{-3} \\
&\cdot \left\{ [E - A(2V_0 + 6Cd^2)]^{3A-5/2} \cdot \Theta [E - A(2V_0 + 6Cd^2)] / \Gamma(3A - 3/2) \right. \\
&- 3 \sum_{m=0}^{(A-3)/2} \frac{C^m R^{2m}}{m! \Gamma(3A - 3/2 - m)} [E - A(2V_0 + 6Cd^2) - CR^2]^{3A-m-5/2} \\
&\quad \cdot \Theta [E - A(2V_0 + 6Cd^2) - CR^2] \\
&+ 3 \sum_{m,m'=0}^{(A-3)/2} \frac{C^{m+m'} R^{2(m+m')}}{m! m'! \Gamma(3A - 3/2 - m - m')} \\
&\quad \cdot [E - A(2V_0 + 6Cd^2) - 2CR^2]^{3A-m-m'-5/2} \\
&\quad \cdot \Theta [E - A(2V_0 + 6Cd^2) - 2CR^2] \\
&- \sum_{m,m',m''=0}^{(A-3)/2} \frac{C^{m+m'+m''} R^{2(m+m'+m'')}}{m! m'! m''! \Gamma(3A - 3/2 - m - m' - m'')}
\end{aligned}$$

$$\begin{aligned}
& \cdot [E - A(2V_0 + 6Cd^2) - 3CR^2]^{3A-m-m'-m''-5/2} \\
& \cdot \Theta [E - A(2V_0 + 6Cd^2) - 3CR^2]
\end{aligned} \tag{9}$$

Here R is given by the same expression as (5).

The eigenvalues are

$$\lambda_{i,j,k} = 2 \left(3 - \cos \frac{2\pi i}{N} - \cos \frac{2\pi j}{N} - \cos \frac{2\pi k}{N} \right)$$

where $(i, j, k = 1, \dots, N)$ and $N = A^{1/3}$.

The correlation between E and T is shown in figure 7. It is similar to the one obtained in the one-dimensional case. In practice, in both cases, the relation between E and T looks like that of an ideal classical gas $T = 3/2E$, but with a different slope because of the presence of an interaction.

4. Discussion and conclusions

We have worked out the properties of an excited system of nucleons with respect to its energy. We introduced a classical model which is aimed to describe a fragmenting nucleus considered as a disordered system. In this model the nucleons occupy finite phase space cells. We have shown in former work that this approach reproduces very successfully the fragment size distributions and related observables predicted by bond percolation models and experimentally observed, hence the properties related to a second order phase transition corrected for finite size effects.

Our interest in the thermodynamic properties of the system was triggered by recent experimental results which indicate that there may exist a first order phase transition in the fragmentation process. The coexistence of phase transitions of first and second order could be explained by the fact that first order transitions become second order transitions at the critical point. The universality properties of the fragment size distributions may reflect the existence of events which lie at the critical point and in its neighbourhood. We used our model in order to construct the microcanonical partition function, taking into account the short range nuclear and long range Coulomb interactions between all the nucleons. It comes out of our calculations that we do not find the plateau of constant temperature in the caloric

curve which characterises a first order transition. This is the case for numerical simulations with different nuclear interactions and also for a simplified analytical approach which leads to a steady increase of the temperature with increasing energy. In numerical simulations we faced the problem that part of the generated configurations do not correspond to thermal equilibrium, since we did not select them by means of an appropriate Metropolis Monte Carlo procedure. This is the reason for which we implemented an analytical approach which implies thermodynamical equilibrium by construction. In order to ensure an analytical expression for the partition function which shows explicitly the behaviour of the caloric curve, we introduced a simplified two-body potential. This potential reproduces the qualitative behaviour of the realistic interaction used in numerical simulations.

The reason for the failure of the present model with respect to the presence of a phase transition are not clear. We suspect that the concept of cells in space introduces a rigid structure which leads to a system closer to a disordered crystal than to a liquid which may vaporize when the excitation energy is high enough. One may of course relax this constraint and possibly, at the same time, select those configurations which correspond to equilibrium. But then the new approach should also reproduce the fragment size distributions which are so nicely obtained in our present approach.

It is our aim to investigate this point in the future and confront it with the outcome of cellular automata techniques which introduce a dynamical description through an explicit time-dependence.

Aknowledgments

The authors would like to thank Prof. D. Gross for fruitful comments and advices. One of us (J.R.) acknowledges interesting discussions with A. Bonasera, J. Polonyi and P. Simon and the help of P. Oswald for the completion of numerical calculations.

References

- [1] J. HUBELE ET AL. — *Phys. Rev.* **C46** (1992) R1577
- [2] U. LYNEN ET AL. — *Nucl. Phys.* **A545** (1992) 329c
- [3] P. CREUTZ ET AL. — *Nucl. Phys.* **A556** (1993) 672
- [4] P. DÉSESQUELLES ET AL. — *Phys. Rev.* **C48** (1993) 1828
- [5] A. SCHÜTTAUF ET AL. — GSI preprint 96-26, June 1996
- [6] X. CAMPI — *J. Phys. A : Math. Gen.* **19** (1986) L917 ; *Phys. Lett.* **B208** (1988) 351
X. CAMPI, H. KRIVINE — Contribution to the International Workshop on Dynamical Features of Nuclei and Finite Fermi Systems, Sitges, Spain (1993) (World Scientific, Singapore)
- [7] B. ELATTARI, J. RICHERT, P. WAGNER, Y.M. ZHENG — *Phys. Lett.* **B356** (1995) 181
- [8] B. ELATTARI, J. RICHERT, P. WAGNER, Y.M. ZHENG — *Nucl. Phys.* **A592** (1995) 385
- [9] J. POCHODZALLA ET AL. — *Phys. Rev. Lett.* **75** (1995) 1040
- [10] S. ALBERGO, S. COSTA, E. COSTANZA, A. RUBBINS — *Nuovo Cimento* **A89** (1985) 1
- [11] X. CAMPI, H. KRIVINE, E. PLAGNOL — “Remarks on a determination of the nuclear caloric curve”, preprint IPNO/TH 96-17
- [12] P. FINOCCHIARO, M. BELKACEM, J. KUBO, V. LATORA, A. BONASERA — *Nucl. Phys.* **A600** (1996) 236
- [13] S. PRATT — *Phys. Lett.* **B349** (1995) 261
- [14] A. GUARNERA, M. COLONNA, PH. CHOMAZ — *Phys. Lett.* **B373** (1996) 267 and refs. quoted therein
- [15] D.H.E. GROSS — *J. Phys. Soc. Japan* **54** (1985) 392 ; *Rep. Prog. Phys.* **53** (1990) 605
- [16] H.W. BARZ, J.P. BONDORF, R. DONANGELO, H. SCHULZ — *Phys. Lett.* **B169** (1986) 318

- [17] Y.M. ZHENG, J. RICHERT, P. WAGNER — *Chinese J. Nucl. Phys.* **17** (1995) 215
- [18] Y.M. ZHENG, J. RICHERT, P. WAGNER — *J. Phys.* **G22** (1996) 505
- [19] L. WILETS, E.M. HENLEY, M. KRAFT, A.D. MCKELLAR — *Nucl. Phys.* **A282** (1977) 341
- [20] R.J. LENK, T.J. SCHLAGEL, V.R. PANDHARIPANDE — *Phys. Rev.* **C43** (1990) 372
- [21] R.W. GERLING, A. HÜLLER — *Z. Phys.* **B90** (1993) 207
- [22] G. ARFKEN — *Mathematical methods for physicists*, New York, London, Academic Press 1985

Figure captions

Fig. 1a: $S(E) = \ln Z(E, A, d)$ as a function of E/A for $A = 216$ and $d = 3$ fm.

Fig. 1b: $(\partial S/\partial E)_V^{-1}$ as a function of E/A ($V = Ad^3$ is the volume of the system).

Fig. 2: $(\partial S/\partial E)_V^{-1}$ as a function of E/A for different values of d ($V = Ad^3$ is the volume of the system) ; the dashed line corresponds to the case where S is averaged over different values of d (see text).

Fig. 3: $S(E)$ and $(\partial S/\partial E)_V^{-1}$ as a function of E/A for $d = 3$ fm with the interaction taken from ref. [20].

Fig. 4: Evolution of the partition $Z(E)$ and fragment multiplicities as a function of E/A . See text. $Z(E)$ is represented in arbitrary units.

Fig. 5: Comparison between the exact (4a) and approximate (6a) expressions of the canonical partition function. The quantities which are represented correspond to the product of error functions in (4a) and the term in brackets in (6a). See text.

Fig. 6: $s(E) = \ln Z(E, A, d)/A$ and temperature T as a function of E/A for $d = 3$ fm and $A = 125$ (1 dimensional system). See text. The parameters are the same as in Fig. 5.

Fig. 7: Same as Fig. 6 for a 3 dimensional system ($A = 5^3$).

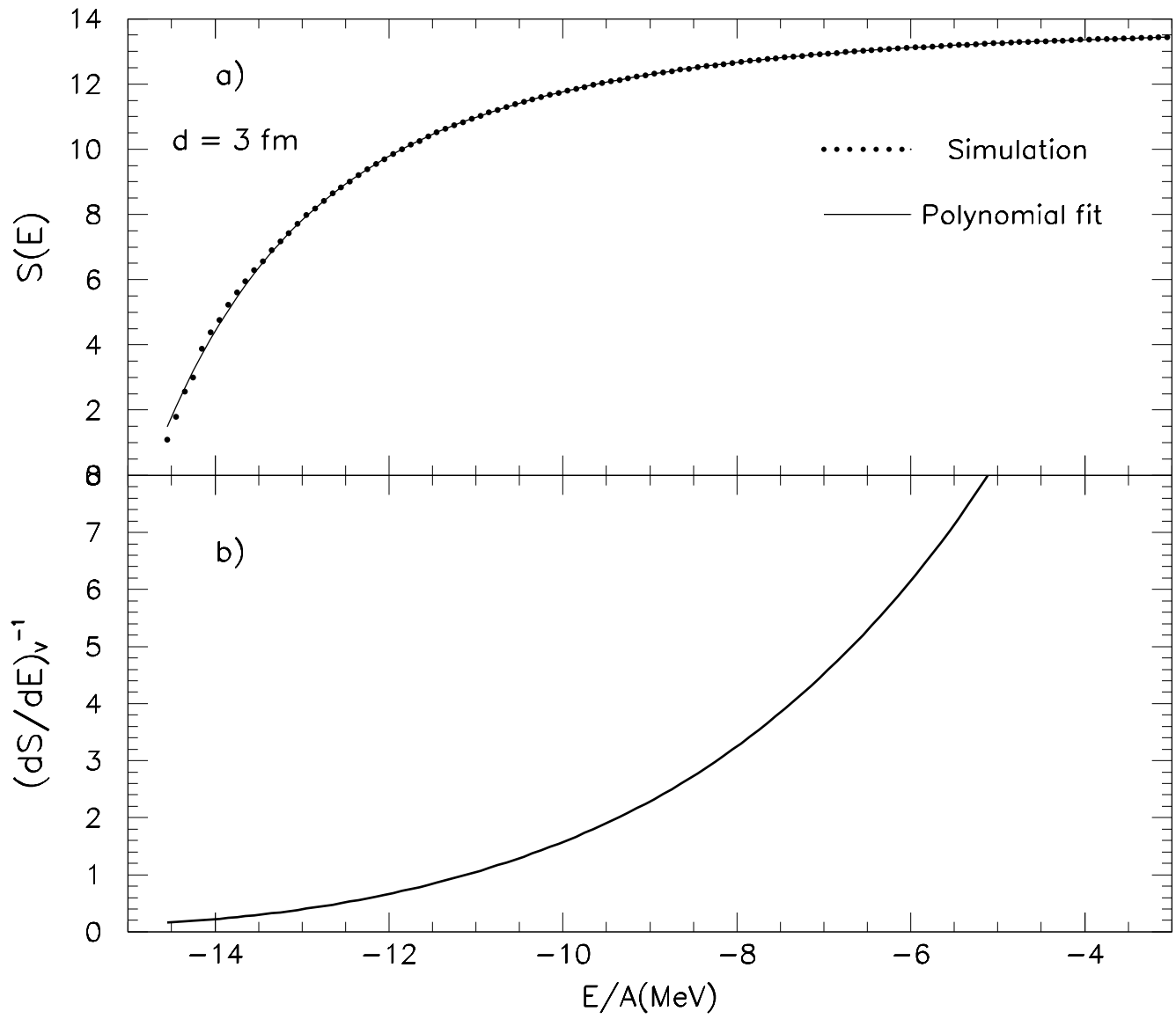


fig.1

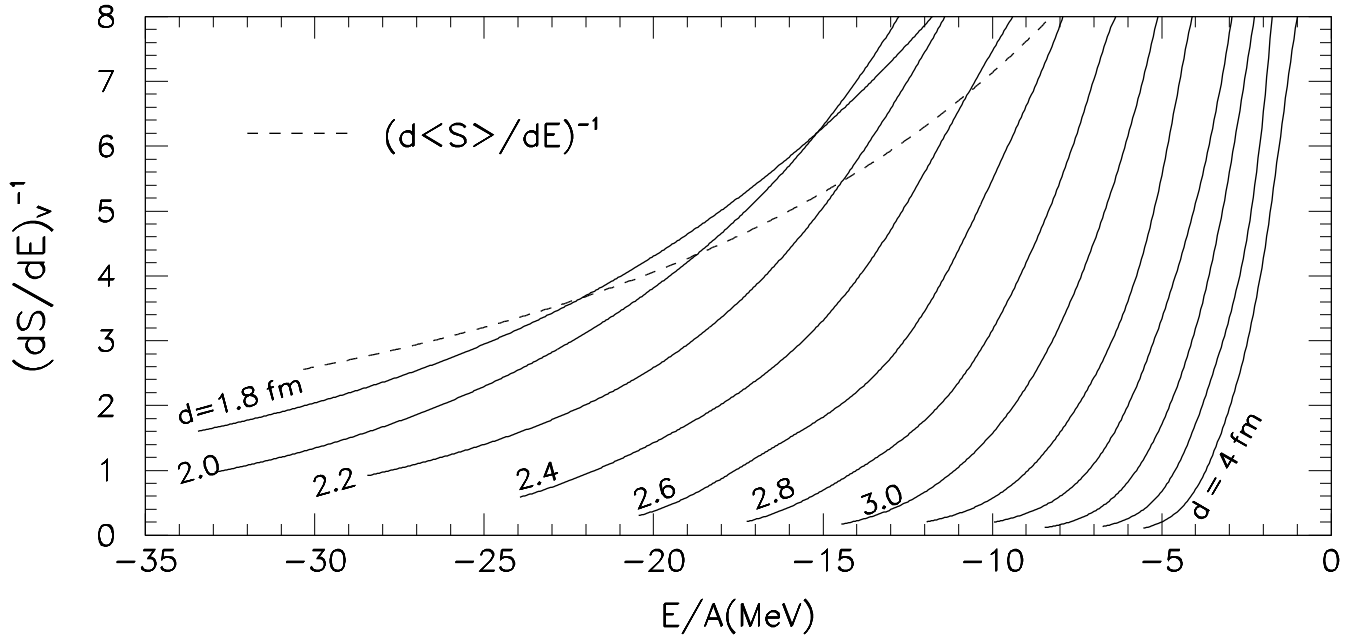


fig.2

d = 3 fm

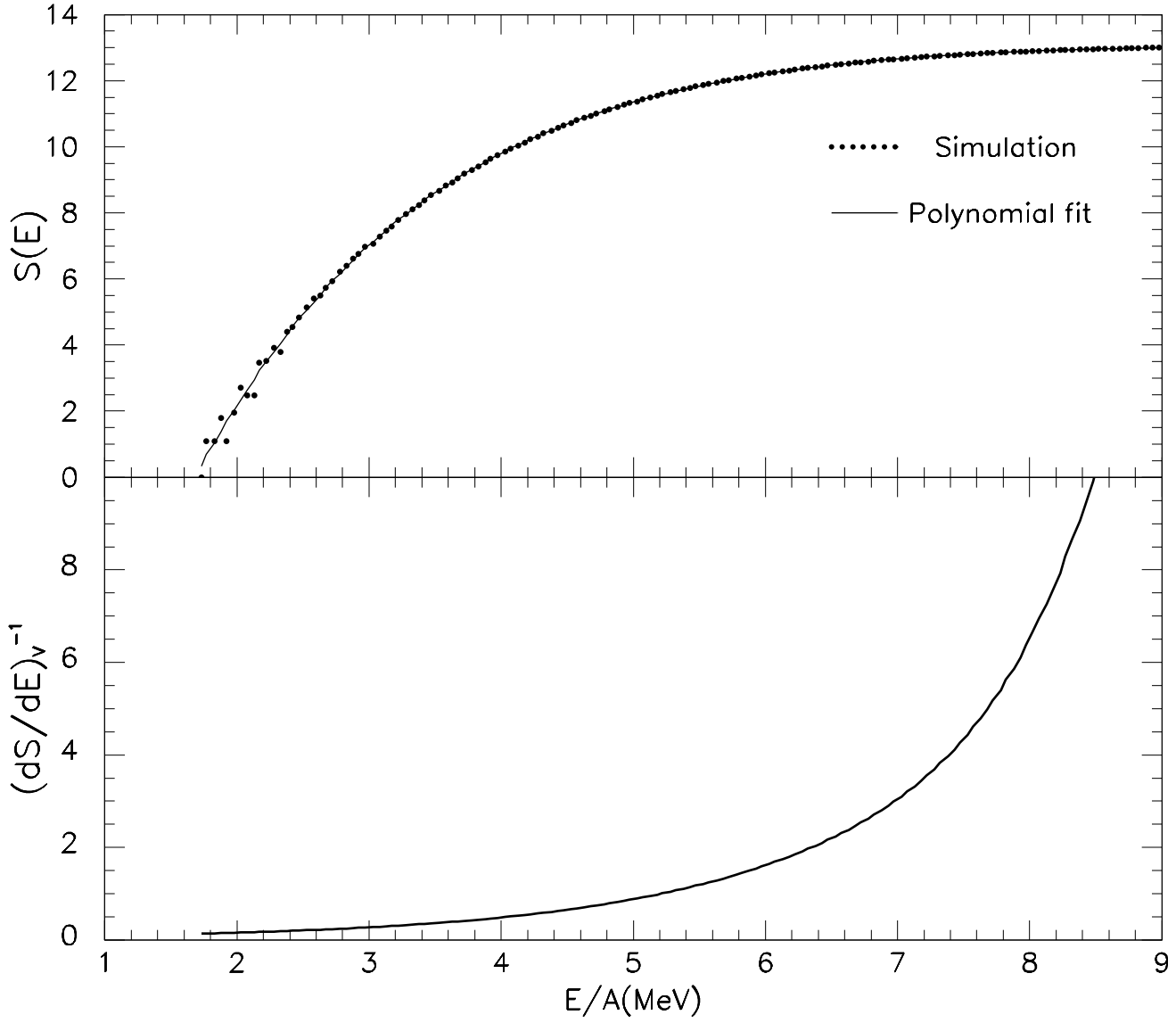


fig.3

d = 3 fm

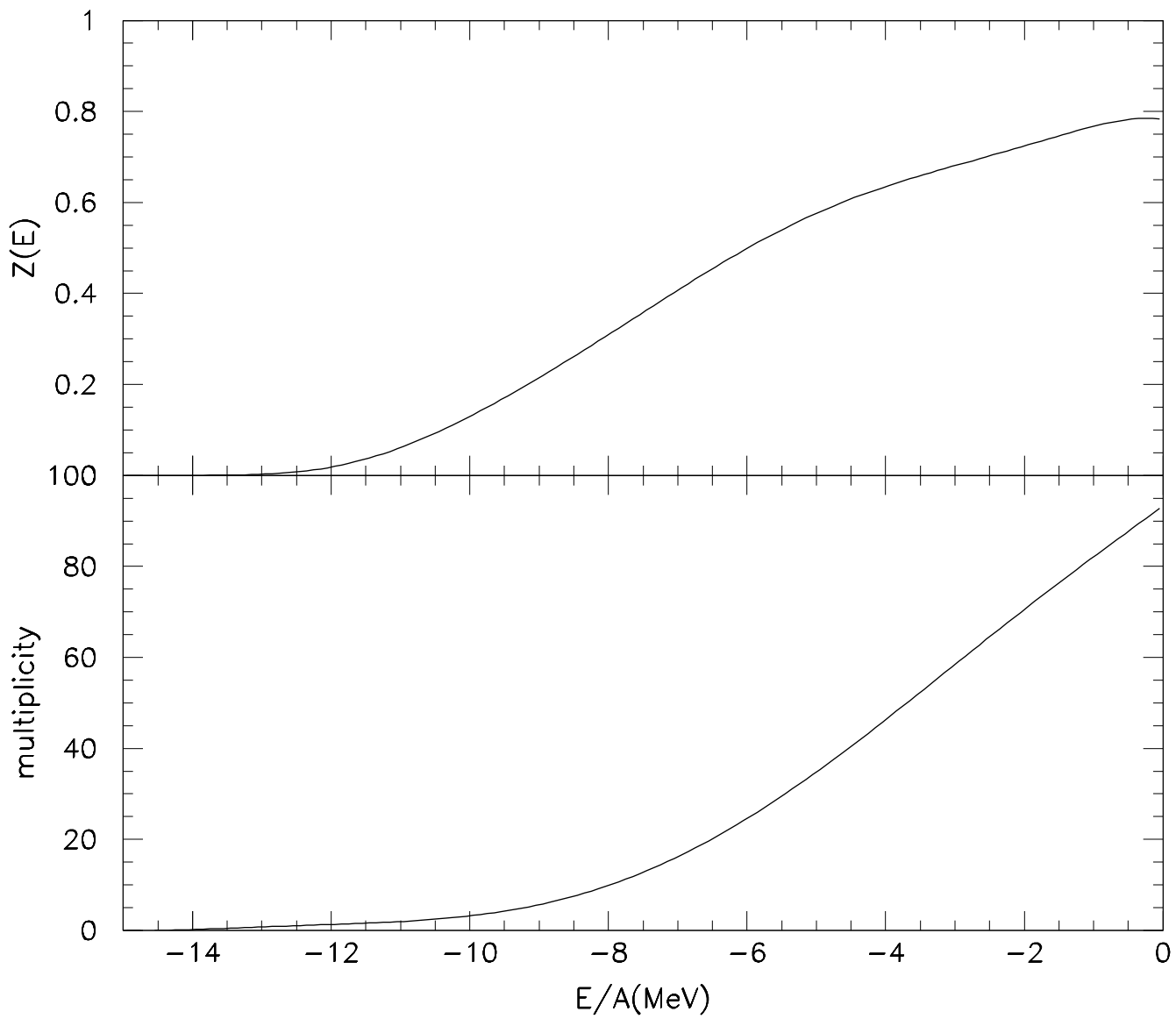


fig.4

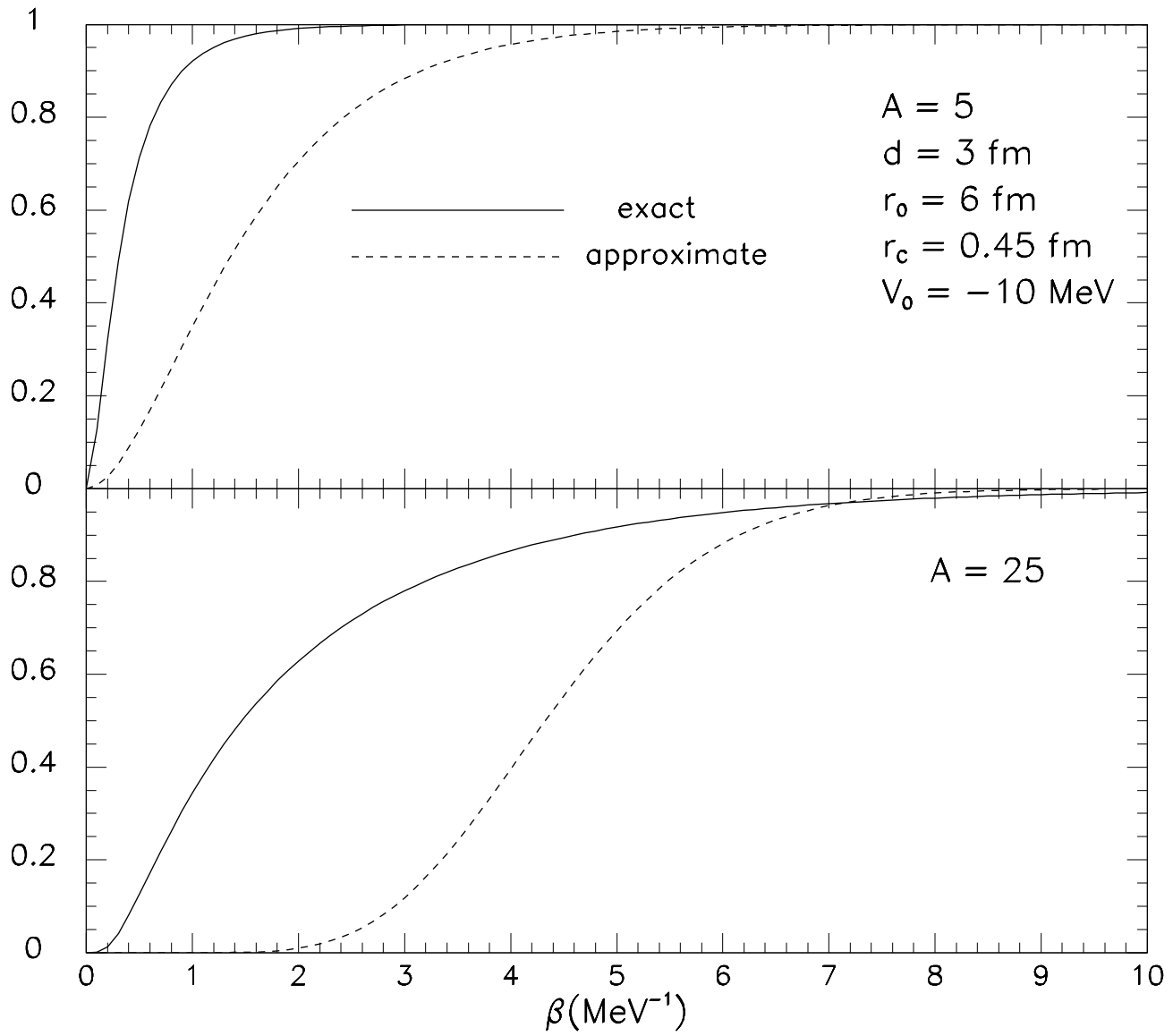


fig.5

1-dimensional case $A = 125$

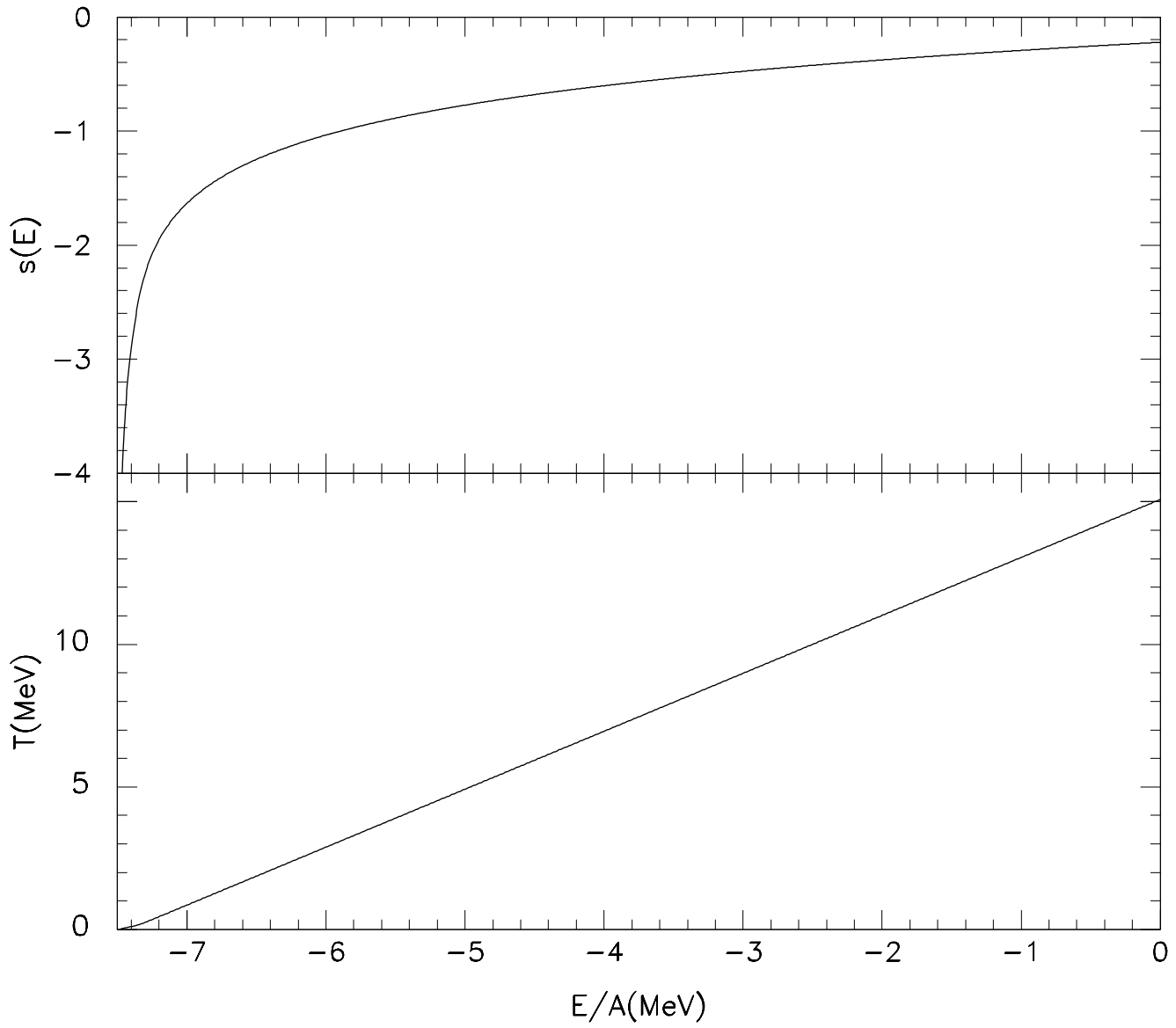


fig.6

3-dimensional case $A = 125$

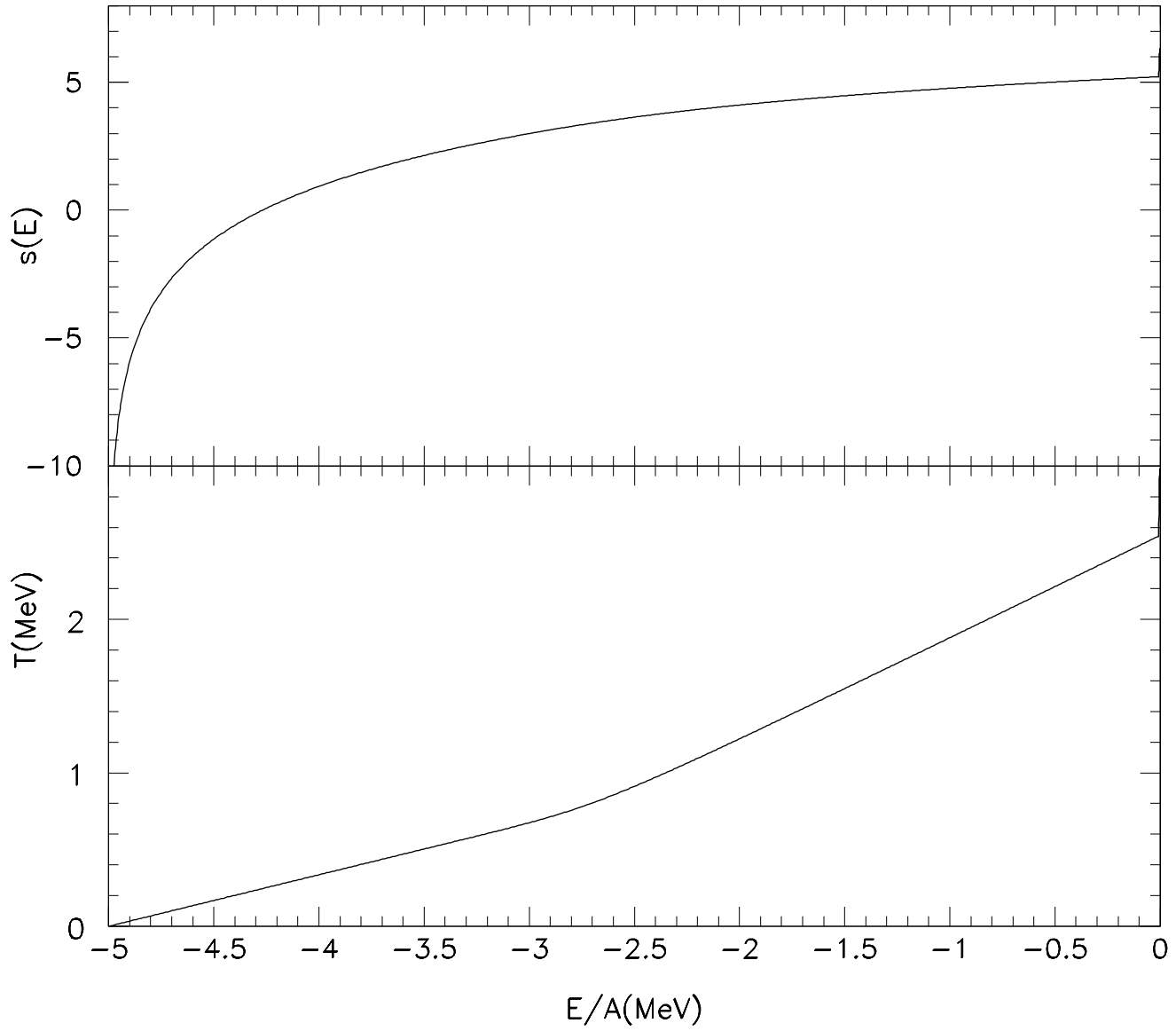


fig.7